J Mater Sci: Mater Med (2008) 19:2691–2697
DOI 10.1007/s10856-008-3391-8

Osteoblast cell response to β-tricalcium phosphate scaffolds with controlled architecture in flow perfusion culture system

Xiang Li · Dichen Li · Lin Wang · Bingheng Lu · Zhen Wang

Received: 29 October 2007 / Accepted: 18 January 2008 / Published online: 19 February 2008

Abstract Porous β-tricalcium phosphate (β-TCP) scaffolds with controlled architecture and improved mechanical properties were fabricated by combining the gel-casting and rapid prototyping techniques. The pore morphology, size, and distribution of the β-TCP scaffolds were characterized using a scanning electron microscope. The porosity of the resulting scaffolds with pore size range from 300 to 500 μm was 46%. The average compressive strength was 16.1 MPa. X-ray diffraction was used to determine the crystal structure and chemical composition of scaffolds. The result indicated that the sintering process has not changed the composition of β-TCP. Flow perfusion culture system was developed in our lab to improve mass transfer for seeded cells. For scaffold/cell constructs cultured under flow perfusion for 4, 8, and 16 days, there was greater scaffold cellularity and alkaline phosphatase activity compared with static culture condition. These results indicated that flow perfusion culture system had evident effects on osteoblast viability and functions in vitro.

X. Li · D. Li · B. Lu
State Key Lab for Manufacturing Systems Engineering, Xi'an Jiaotong University, Xi'an 710049, China

X. Li (✉)
Department of Mechanical Engineering, The Institute of Advanced Manufacturing Technology, Xi'an Jiaotong University, Xi'an 710049, China
e-mail: Xiangliwj@yahoo.com.cn

L. Wang · Z. Wang
Xijing Hospital, The Fourth Military Medical University, Xi'an 710032, China

1 Introduction

One of the most attractive bioceramics, β-tricalcium phosphate (β-TCP), has been widely used in orthopedic applications due to its excellent biocompatibility, osteoconductivity, and osteoinductivity [1–5]. For use as tissue scaffolds, β-TCP has been developed into porous structure. For instance, porous β-TCP blocks with four different macropore sizes (pore larger than 50 μm) were synthesized using calcium phosphate emulsions, and characterized by optical, geometrical, gravimetric, and radiological methods [6], β-TCP scaffolds with designed, three-dimensional geometry and mesoscale porosity have been fabricated by direct-write assembly techniques [7], and the porous β-TCP scaffolds seeded with bone marrow stromal cells were used to repair canine mandibular bone defects [8]. Previous studies have demonstrated that a 3D interconnected porous structure is necessary to allow cell ingrowth and reorganization in vitro and provide the necessary space for neovascularization from surrounding tissues in vivo [9–12]. Rapid prototyping (RP) techniques have been found to be advantageous for tissue engineering scaffold fabrication due to their ability to address and overcome the problems of uncontrollable microstructure and the feasibility issues of complex three-dimensional structures found in conventional processing techniques [13–16]. The application of CAD strategies in conjunction with RP fabrication can allow scaffolds with highly uniform pore morphologies, pore sizes, porosity and complete pore interconnectivity to be realized with unprecedented accuracy and consistency [14].

Gel casting is a common technique for fabricating ceramic bodies with high mechanical strength by means of in situ polymerization through which a macromolecular network is created to hold the ceramic particles together.

It has been adapted for the manufacture of porous bioceramics from foamed suspensions, but it usually results in a structure of poorly interconnected pores, and non-uniform pore distribution [17–19]. The cytotoxicity tests indicated that gel-casting porous hydroxyapatite (HA) can be considered as a potential candidate material for applications such as bone implants [18]. In vitro culture of standardised hydroxyapatite scaffolds fabricated by RP technique demonstrated that cells were attached to all scaffold surfaces. And in vivo evaluation revealed that bone formation in all scaffolds after 4–6 weeks implantation [15]. It has long been known that the supply of oxygen and soluble nutrients becomes critically limiting for the in vitro culture of 3D tissues. Mass transport limitation is one of the greatest challenges to 3D scaffolds cultured under static condition. A dynamic culture condition, flow perfusion culture system, can reduce the mass transfer limitations both at the construct periphery and within its internal pores and enhance growth, differentiation and mineralized matrix deposition by bone cells [20]. The growth and osteoblastic function of pre-osteoblastic cells seeded on porous scaffolds were examined for four different culturing methods: a flow system, a spinner flask, a rotary vessel, and static culture. The results demonstrated that culturing techniques that utilize fluid flow, and in particular the flow perfusion system, improve the properties of the seeded cells over those maintained in static culture [21]. The effect of culturing conditions (static and flow perfusion) on the proliferation and osteogenic differentiation of rat bone marrow stromal cells seeded on porous scaffolds was investigated. And the results suggested that flow perfusion culture enhances the osteogenic differentiation of marrow stromal cells and improves their distribution in three-dimensional, starch-based scaffolds [22].

In this study, by combining gel casting and RP techniques, we fabricated β-TCP porous scaffolds with controlled architecture. Firstly, the negative molds were designed using a CAD software and produced on a stereolithography apparatus. Ceramic slurry was then cast into the resin molds. The porous scaffolds were obtained after removing the resin molds via sintering process. The structural and mechanical properties of the porous scaffolds were investigated. The growth and function of osteoblasts seeded on resulting scaffolds were examined under static culture and flow perfusion culture system developed in our lab.

2 Materials and methods

2.1 Scaffold fabrication

The processing technique used for fabrication of the porous scaffolds involves the preparation of thermosetting ceramic slurry, a mixture consisting of β-TCP powder, distilled water, dispersion agent, and water soluble monomers. β-TCP powder was obtained from Edward Keller Limited (Shanghai China). This powder has an average particle size of 2.3 μm with a surface area of 1–6 m^2/g. The monomers used in our gelcasting experiments were methacrylamide and a crosslinking agent N,N'-methylenbis(acrylamide). A 25% aqueous solution of ammonium polymethacrylate was used as a dispersant. Ammonium persulphate and N,N,N,N, tetramethylethylenediamine were used as the initiator and catalyst, respectively. All these chemicals were purchased from Sigma-Aldrich Corporation. Molds for gelcasting scaffolds were designed using a commercial CAD software (Unigraphics NX, EDS) and produced on a stereolithography apparatus. The slurry was ball-milled for 12 h and subsequently deaired under vacuum until no further release of air bubbles from the sample. After added with catalyst and initiator, the slurry was cast into resin molds produced and then kept for an hour at a temperature of 60°C, in order to polymerise the monomers and thus stabilise the green body. After polymerization, the samples were dried in air for 48 h and subsequently heated in air in an electric furnace with a heating rate of 1°C/min from room temperature to 600°C, holding 180 min at 600°C to burn out resin molds, then sintered with a heating rate of 5°C/min to 1150°C.

2.2 Characterization of the scaffolds

XRD was used to characterize the crystallinity, chemical composition, and structure of the materials. XRD experiments were performed on both as-purchased β-TCP powder and the sintered samples after being crushed to powders, using a Rigaku D/MAX-3C powder diffractometer with mono-chromatic CuKα radiation. The XRD data were collected employing a step scan of $2\theta = 0.02$ and 5 s preset time under 40 kV and 20 mA excitation. The macro- and microstructures of the resulting scaffolds were examined with Scanning electron microscopy (SEM, S-3000, HITACHI, Japan). The porosity of the sample was calculated by measuring its dimensions and weight. Compression tests were conducted with an Instron 5848 material testing system using a 10-kN load-cell (Canton, MA, USA). The crosshead speed was set at 0.5 mm/min, and the load was applied until the scaffold was cracked.

2.3 Osteoblast isolation and culture

Osteoblastic cells were isolated from the femurs of young (3–5 days old) New Zealand white rabbits. The calvaria were isolated, and all connective tissues were carefully

removed. The parietal bones were minced into pieces measuring about 1 × 1 mm^2 using sterile surgical scissors. Osteoblasts were isolated by an enzyme solution containing 1.37 mg/ml collagenase type I (Sigma) and 0.5 mg/ml trypsin (Sigma). Following 30 min of incubation, the released cells were discarded to prevent contamination with other cell types. The minced bones were redigested with the enzyme solution for 30 min, and the supernatant was transferred to the culture medium, Dubecco's Modified Eagle's Medium (DMEM) (Gibco) supplemented with 10% fetal bovine serum (FBS) (Jingke Biotechnology, Beijing, China), 100 μg/ml streptomycin (Jingke), L-ascorbic acid (50 g/ml) (Sigma), sodium-glycerophophate (10 mM) (Sigma), 100 U/ml penicillin (Jingke), and dexamethasone (10 nM) (Sigma). This process was repeated three times, and then finally the collected solution was centrifuged for 10 min at 1500 rpm. Cells were plated into tissue culture flasks and cultured in a humidified incubator at 37°C with 5% CO2. The primary osteoblasts were then left until confluence was reached.

2.4 Seeding of cells into scaffolds

The fabricated scaffolds were sterilized by ethylene oxide gas and soaked in the culture medium for 12 h. Cell seeding was performed by addition of a concentrated cell suspension (2 × 10^6 cells/ml) in a drop-wise manner to ensure cell loading directly onto the pre-wetted scaffolds. The volume of the cell suspension added to each scaffold was 0.5 ml. The cells were allowed to adhere to the scaffolds for 2 h and then the cell/scaffold constructs were placed in 6-well plates, covered with 10 ml of media, incubated at 37°C in a 5% CO_2, 100% relative humidity incubator. Seeded scaffolds were incubated for further attachment overnight. The following day seeded scaffolds were placed into fresh six-well plates for static conditions or into the flow perfusion system for 4, 8, and 16 days.

2.5 Flow perfusion culture system

A flow perfusion culture system was developed in our lab. It consisted of eight flow chambers machined in a block of polymethylmethacrylate (Fig. 1). Each flow chamber contained a β-TCP scaffold which was fixed in silicone rubber block to ensure the flow path was only through the scaffold. Flow through each chamber was driven by a multichannel peristaltic pump with each flow chamber on its own independent pumping circuit to ensure a consistent, controllable flow rate to each flow chamber. All flow chambers drew media from a common reservoir. The entire flow circuit was connected with silicon tubing, which has a high permeability to both carbon dioxide and oxygen thereby ensuring adequate gas equilibration with the surrounding incubator air. Before use, the entire culture system was sterilized by ethylene oxide. For these experiments, culture media was pumped continuously at a flow rate of 0.5 ml/min through the cell/scaffold constructs and then recirculated back to the reservoir.

2.6 Scanning electron microscopy

Scanning electron microscopy was used to monitor cell attachment, morphology and mineral production by osteoblasts. Samples were removed from culture and rinsed three times with PBS after 16 days incubation. Subsequently, fixation was carried out for 2 h at 4 in 2% glutaraldehyde in 0.1 M sodium cacodylate buffered solution. Samples were then washed with cacodylate buffer 0.1 M, pH 7.4 three times and dehydrated in a graded series of ethanol, and dried by tetramethylsilane. The dried samples were glued onto aluminum stubs, sputter-coated with gold and examined using a SEM (S-3000, HITACHI, Japan) at an accelerating voltage of 20 kV.

2.7 Alkaline phosphatase activity

Alkaline phosphatase (ALP) activity of the cells was measured as an early marker of the maintenance of the osteoblastic phenotype using an ALP substrate kit. This colorimetric assay is based on the conversion of *p*-nitrophenyl phosphate (P-NPP) into *p*-nitrophenol (P-NP) in the presence of ALP, where the rate of P-NP production is proportional to ALP activity. Briefly, Cells were rinsed three times with PBS followed by trypsinization and then scraped in lysis buffer (250 mm NaCl, 0.1% Triton X-100,

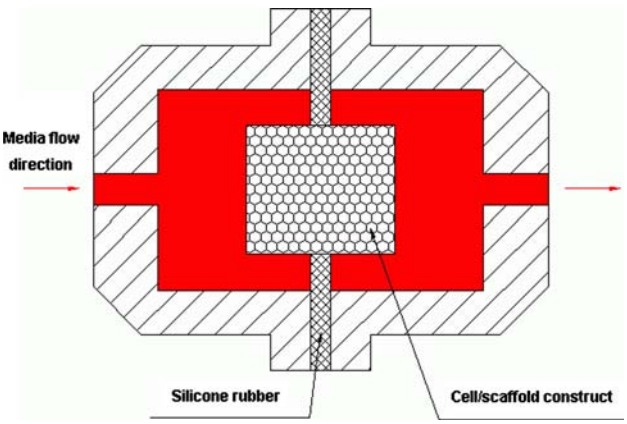

Fig. 1 Schematic of an individual flow chamber of flow perfusion culture system

50 mm Hepes, pH 7.5). This was followed by three cycles of freezing and thawing. The cell lysates were collected and stored at −70°C in a freezer. On thawing, a volume of the sample (100 ml) was added to 400 ml of P-NPP substrate and buffer solution mixture and incubated at 37°C for 30 min. The reaction was then stopped by adding 500 ml of 0.4 N sodium hydroxide. ALP activity was determined at 410 nm using *p*-nitrophenyl phosphate (Sigma) as the substrate and expressed as μmol/hr/mg of protein/g of scaffold.

2.8 MTT assay

Cell proliferation was assessed using a methylthiazol tetrazolium (MTT) assay. Briefly, 800 μl serum free medium and 80 μl MTT solution (5 mg/ml in PBS) were added to each sample. After 4 h of incubation at 37°C in a fully humidified atmosphere at 5% CO_2 in air, MTT was taken up by active cells and reduced in the mitochondria to insoluble purple formazan granules. Subsequently, the medium was discarded and the precipitated formazan was dissolved in DMSO, and after 10 min of slow shaking the absorbance was read at 570 nm using a Bio-Rad 500 spectrophotometric microplate reader. Tissue culture plate served as controls. Five specimens were tested for each incubation time and each test was performed in triplicate. Results were reported as optical density units.

2.9 Statistical analyses

Statistical analysis of data for cell proliferation was carried out by one-way analysis of variance (ANOVA) to determine the presence of any significant difference among sample means of the groups, followed by Tukey's test for multiple comparisons to determine the values that were significantly different at $P < 0.05$.

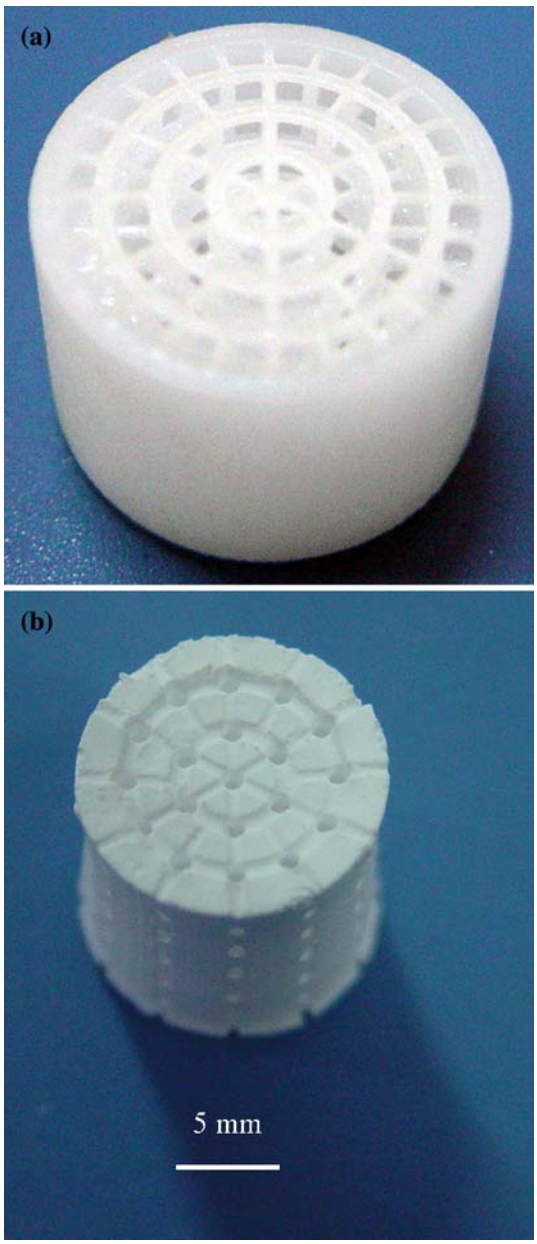

Fig. 2 (**a**) Resin mold produced by stereolithography; (**b**) the resulting scaffolds with controlled architecture

3 Results and discussion

Figure 2a shows the resin mold produced by stereolithography. Before using, molds were cleaned with isopropanol alcohol. After burning out the resin molds, the resulting scaffolds were obtained (shown in Fig. 2b). The fabricated β-TCP scaffolds exhibited excellent shape tolerance, without distortion or cracking. Pure β-TCP undergoes phase transition to α-TCP at about 1200°C [16]. Thus preserving the phase composition and crystalline structure of β-TCP after sintered should be examined. Figure 3 shows the XRD patterns of the β-TCP powder as received and the material after being sintered at 1150°C. The XRD peaks of both diffraction patterns agree well with those of standard β-TCP in the diffraction file (Card No. 09-0169). This indicates that the sintering process has not changed the composition of β-TCP. The interconnected channels with mean diameters of about 300 μm in *X*–*Y* plane and 500 μm in *Z* direction could be realized. Figure 4a shows an internal channel network in a scaffold. Figure 4b shows that the granule structure remains after sintering. The porosity of the resulting scaffolds was 46%. The average compressive strength was 16.1 MPa ($n = 5$).

Osteoblast proliferation on the surface of the scaffolds and inside the channel network was also investigated by SEM analysis. Figure 5 shows the micrographs of cell attachment onto the scaffold under static culture and flow perfusion culture system after 8 and 16 days of incubation. From the micrographs, we can see that after 8 days culture of flow perfusion culture, the cells were more spread and appeared to be surrounded by a thicker extracellular matrix (shown in Fig. 5a), and the cells started migrating into the macrochannels (shown in Fig. 5b). For static culture, the cells accumulated mainly on the surface of the scaffolds and exhibited a thin layer of extracellular matrix (shown in Fig. 5c). After 16 days of flow perfusion culture, cells migrated throughout the scaffold, and the dense matrix was not only present on the surface but also extended throughout the scaffold (shown in Fig. 5d). Within the cell/scaffold constructs, the homogeneous cell distribution can be seen (shown in Fig. 5e, f). Large number of cells and mineralized matrix almost covered the open macrochannels in static culture conditions for 16 days (shown in Fig. 5g).

The osteoblastic phenotype expression of the cells on the scaffolds was assessed by measuring the ALP expressed by the cells after culturing for up to 16 days, since the ALP activity is regarded as an important marker characterizing osteoblastic or osteogenic cells undergoing the differentiation step. Levels of ALP activity of the cells cultured on β-TCP scaffolds under static culture and flow perfusion culture system are shown in Fig. 6. For both cell culture conditions, the ALP activity of the osteoblasts increased during 16-day culture period. In addition, at all time points the ALP activity was significantly higher in the flow perfusion culture as compared with static culture.

The MTT assay was used to determine osteoblastic cells proliferation on the fabricated β-TCP samples. The optical density (OD) values of cell proliferation on porous β-TCP scaffolds under static culture and flow perfusion culture system after 4, 8, and 16 days are shown in Fig. 7. The increase of cell viability with time during the culture was similar to the increase of the daily glucose consumption in both static and flow perfusion cultures. The increase was much greater under flow perfusion culture compared to static culture. The significant increase was observed from day 4 to day 8 and from day 8 to day 16 in the flow perfusion culture. While under static culture conditions a significant increase was seen from day 4 to day 8 and no increase was seen from day 8 to day 16.

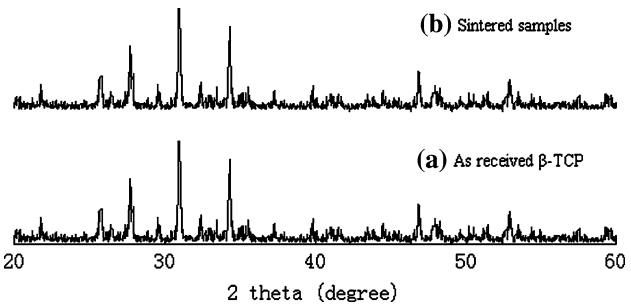

Fig. 3 XRD patterns for (a) β-TCP powder as received; (b) sintered samples

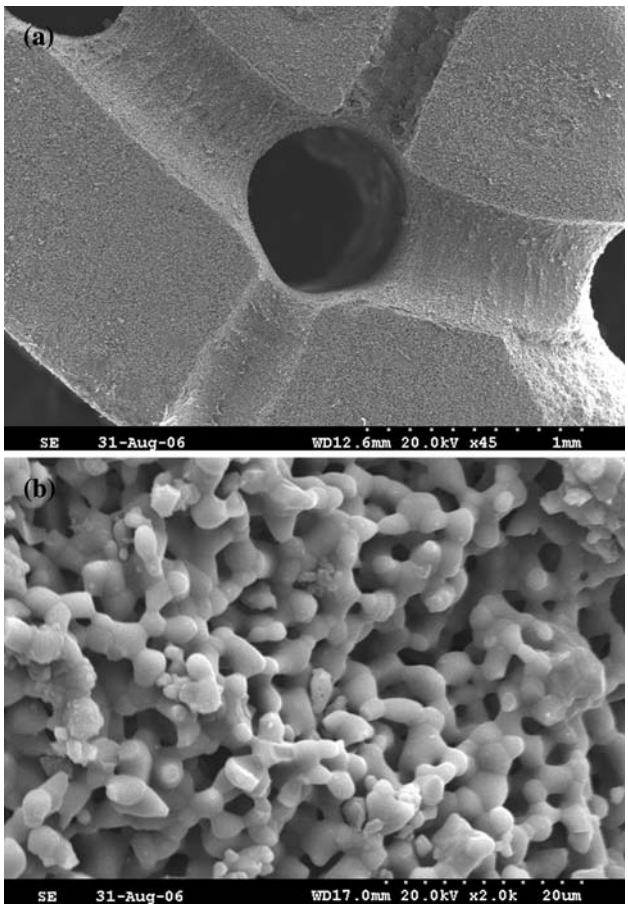

Fig. 4 SEM micrographs for (**a**) a network of interconnected channels; (**b**) detail of the surface morphology

The uneven cell distributions observed in the static culture indicated that the growth of cells in the interior of scaffolds was limited due to poor nutrient diffusion. Various flow perfusion culture systems were utilized to overcome the mass transfer limitations occurred in the cell/scaffold constructs. The perfusion culture system, facilitating supply of nutrients and oxygen to the seeded cells and removal of metabolic products and degradation products from biodegradable scaffolds while producing low levels of shear stresses, showed improved cell viability and functions for tissue regeneration [20–23]. Flow-mediated shear stresses in the range of 0.5–1.5 Pa (5–15 dynes/cm^2) affect osteoblast proliferation as well as production of alkaline phosphatase, indicating that

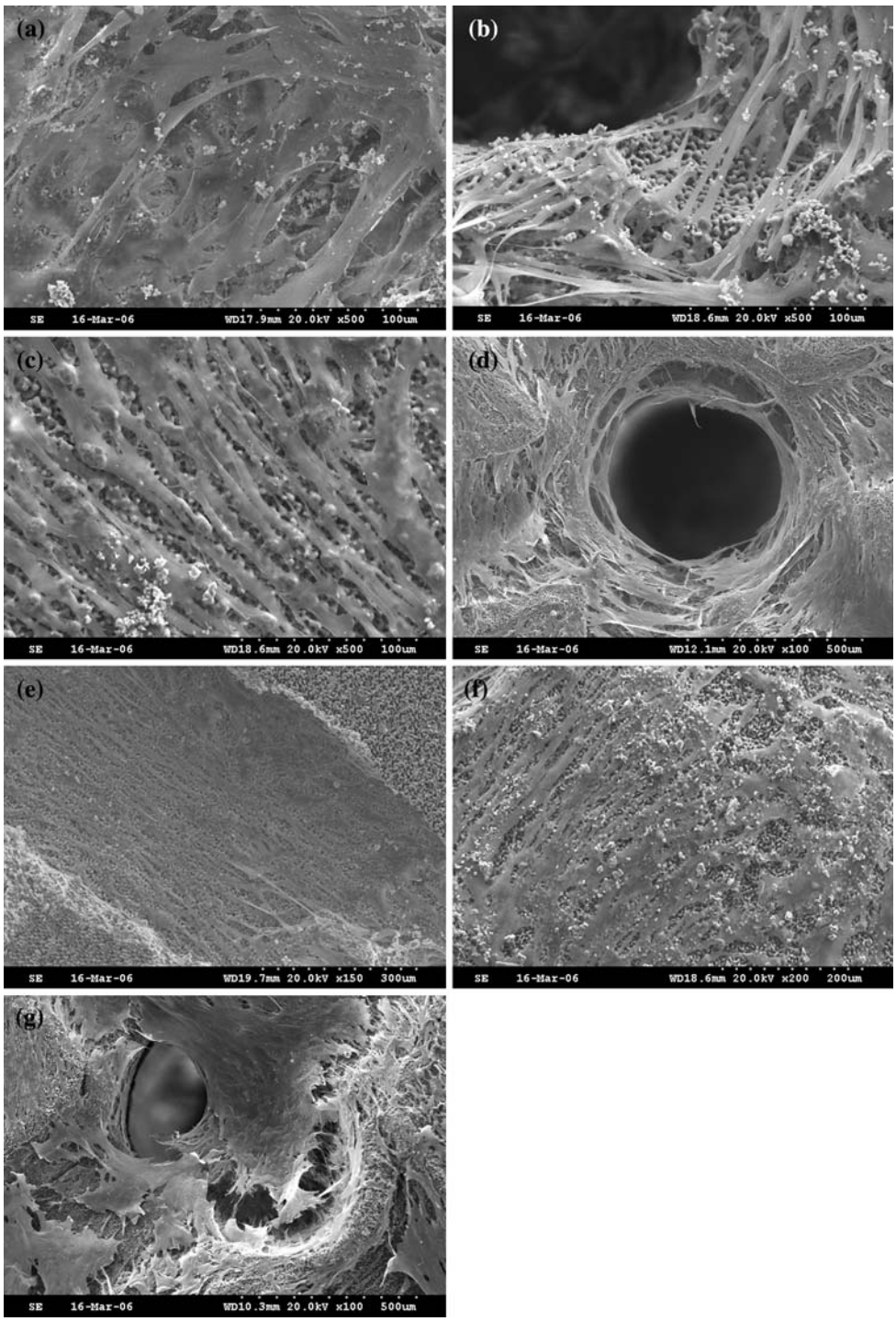

Fig. 5 SEM images of scaffold/cell constructs cultured for 8 and 16 days. (**a**) and (**b**) flow perfusion culture for 8 days; (**c**) static culture for 8 days; (**d–f**) flow perfusion culture for 16 days. Cells were homogeneous distributed within scaffold. And lots of cells migrated throughout the scaffold. (**g**) static culture for 16 days. Large number of cells and mineralized matrix almost blocked the open macrochannels

shear stress is an important regulator of cell function [24, 25]. Results of SEM showed that cells were not damaged, indicating that the shear stresses under flow perfusion system developed in our lab were benefit for the growth and function of osteoblasts. The levels of ALP activity under flow perfusion system were higher than those in the static culture due to the facilitated mass transfer.

4 Conclusions

The β-TCP scaffolds with controlled architecture were fabricated via integrating RP with gel-casting techniques which have the combined advantages of both the techniques. The interconnected macrochannels with the size ranging 300–500 μm were examined by SEM. XRD results showed that the phase and crystallinity of the resulting

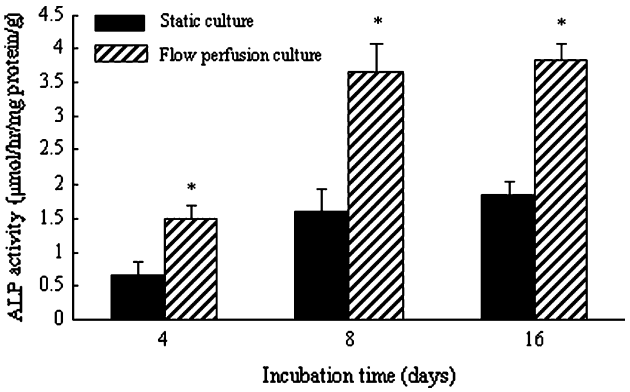

Fig. 6 Alkaline phosphatase activity of osteoblastlike cells after 4, 8, and 16 days under static culture condition or under flow perfusion system. Error bars represent means ± SD. Asterisk (*) indicates a significant difference in alkaline phosphatase activity at day 4, 8, and 16 between static and flow perfusion system ($P < 0.05$)

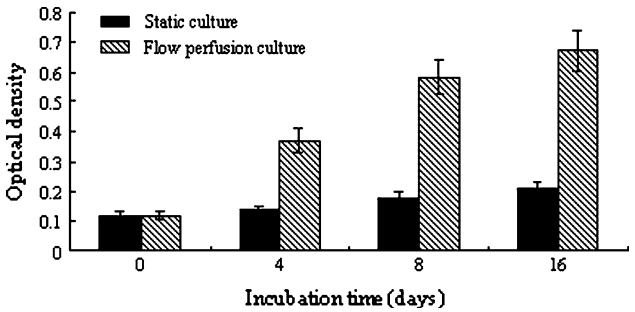

Fig. 7 Cell viability of cell/scaffold constructs over 16 days of culture. There was a continuing increase under both culture conditions. The increase was much greater in the flow perfusion culture than in the static culture ($P < 0.05$)

scaffolds remain unchanged after sintering process. Flow perfusion culture system was developed in our lab to promote growth and osteoblastic function of cells seeded on porous β-TCP scaffolds. The uniform distribution of cells, viability, and higher levels of ALP activity were observed in the flow perfusion culture system.

Acknowledgements The authors would like to thank the National Natural Science Foundation of China (Grant No. 50235020) for their support to this work.

References

1. R.W. Nicholas, T.A. Lange, Clin. Orthop. **306**, 197 (1994)
2. A. Ogose, T. Hotta, H. Hatano, H. Kawashima, K. Tokunaga, N. Endo, H. Umezu, J. Biomed. Mater. Res. **63**, 601 (2002)
3. N. Matsushita, H. Terai, T. Okada, K. Nozaki, H. Inoue, S. Miyamoto, K. Takaoka, J. Biomed. Mater. Res. **70A**, 450 (2004)
4. A. Ogose, T. Hotta, H. Kawashima, N. Kondo, W. Gu, T. Kamura, N. Endo, J. Biomed. Mater. Res. Part B: Appl. Biomater. **72B**, 4 (2005)
5. H.H. Horch, R. Sader, C. Pautke, A. Neff, H. Deppe, A. Kolk, Int. J. Oral Maxillofac. Surg. **35**, 708 (2006)
6. M. Bohner, G.H. van Lenthe, S. Grunenfelder, W. Hirsiger, R. Evison, R. Muller, Biomaterials **26**, 6099 (2005)
7. P. Miranda, E. Saiz, K. Gryn, A.P. Tomsia, Acta Biomater. **2**, 457 (2006)
8. J. Yuan, L. Cui, W.J. Zhang, W. Liu, Y.L. Cao, Biomaterials **28**, 1005 (2007)
9. J.X. Lu, B. Flautre, K. Anselme, P. Hardoiun, A. Gallur, M. Deschamps, B. Thierry, J. Mater. Sci: Mater. Med. **10**, 111 (1999)
10. T.M. Freyman, I.V. Yannas, L.J. Gibson, Prog. Mater. Sci. **46**, 273 (2001)
11. J. Zeltinger, J.K. Sherwood, D.A. Graham, R. Mueller, L.G. Griffith, Tissue Eng. **7**, 557 (2001)
12. F.J. O'brien, B.A. Harley, I.V. Yannas, L.J. Gibson, Biomaterials **26**, 433 (2005)
13. K.F. Leong, C.M. Cheah, C.K. Chua, Biomaterials **24**, 2363 (2003)
14. D.W. Hutmacher, M. Sittinger, M.V. Risbud, Trends Biotechnol. **22**, 354 (2004)
15. C.E. Wilson, J.D. Bruijn, C.A. Blitterswijk, A.J. Verbout, W.J. Dhert, J. Biomed. Mater. Res. **68A**, 123 (2004)
16. M. Lee, J.C.Y. Dunn, B.M. Wu, Biomaterials **26**, 4281 (2005)
17. G. Meng, H. Wang, W. Zheng, X. Liu, Mater. Lett. **45**, 224 (2000)
18. P. Sepulveda, J.G.P. Binner, S.O. Rogero, O.Z. Higa, J.C. Bressiani, J. Biomed. Mater. Res. **50**, 27 (2000)
19. H.R. Ramay, M. Zhang, Biomaterials **24**, 3293 (2003)
20. I. Martin, D. Wendt, M. Heberer, Trends Biotechnol. **22**, 80 (2004)
21. A.S. Goldstein, T.M. Juarez, C.D. Helmke, M.C. Gustin, A.G. Mikos, Biomaterials **22**, 1279 (2001)
22. M.E. Gomes, V.I. Sikavitsas, E. Behravesh, R.L. Reis, A.G. Mikos, J. Biomed. Mater. Res. **67A**, 87 (2003)
23. H.L. Holtorf, J.A. Jansen, A.G. Mikos, J. Biomed. Mater. Res. **72A**, 326 (2005)
24. G.L. Jiang, C.R. White, H.Y. Stevens, J.A. Frangos, Am. J. Physiol. Endocrinol. Metab. **283**, 383 (2002)
25. B. Porter, R. Zauel, H. Stockman, R. Guldberg, D. Fyhrie, J. Biomech. **38**, 543 (2005)